Supplementary figures

Fig. S1

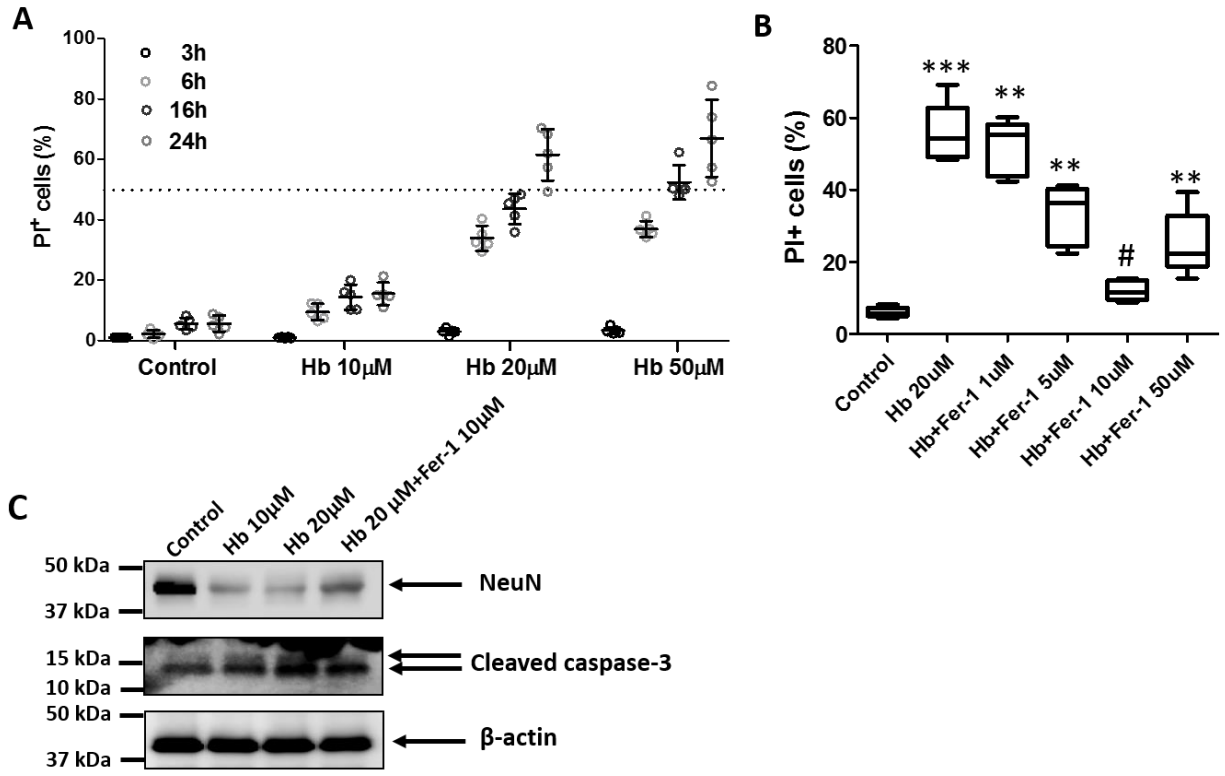

Fig. S1. Time- and dose-dependent hemoglobin-induced cell death in OHSCs is inhibited by Fer-1. (**A**) OHSCs were exposed to different doses of hemoglobin (Hb) for the times shown. Propidium iodide (PI) was added 30 minutes before photomicrographs were taken. Percentage of cell death was determined by fluorescence intensity. (**B**) OHSCs were exposed to vehicle (Control) or 20 μM Hb in the presence or absence of Fer-1 for 16 hours. The percentage of PI-positive cells is shown. **p<0.01, ***p<0.001 vs. Control; #p<0.05 vs. Hb. (**C**) OHSCs were treated as indicted, and brain tissue was homogenized for Western blotting. β-actin served as a loading control. Results are shown as dot plots (mean ± SD) or box-and-whisker plots (the middle horizontal line within the box represents the median; boxes extend from the 25th to the 75th percentile; and the whiskers

represent 95% confidence intervals). One-way ANOVA followed by Dunn's multiple comparison post-test was used. n=5-8 slices. Results are from at least three independent experiments.

Fig. S2

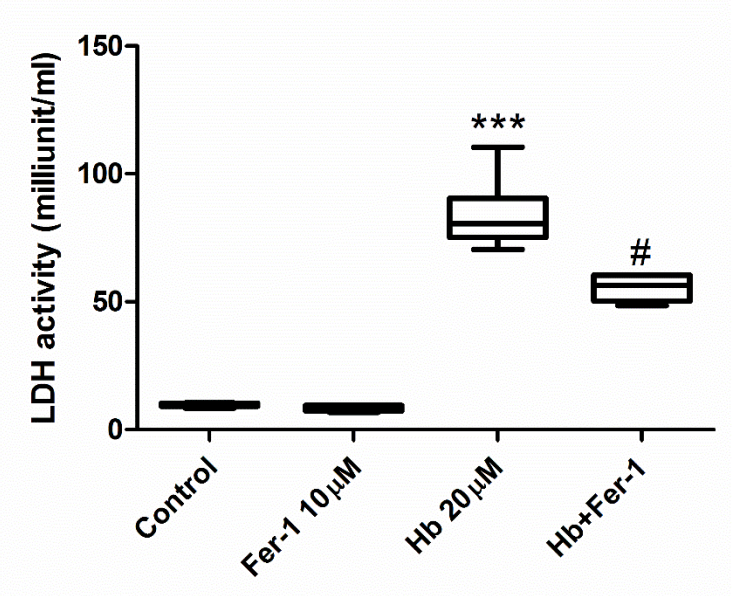

Fig. S2. Fer-1 reduces neuronal death in striatal slice cultures. Striatal slice cultures were exposed to vehicle (Control), 10 μM Fer-1, or 20 μM hemoglobin (Hb) in the presence or absence of Fer-1 for 16 hours. Culture medium was collected and concentrated for use in the lactate dehydrogenase (LDH) assay. ***$p<0.001$ vs. Control; #$p<0.05$ vs. Hb. Results are shown as box-and-whisker plots (the middle horizontal line within the box represents the median; boxes extend from the 25th to the 75th percentile; and the whiskers represent 95% confidence intervals). One-way ANOVA followed by Dunn's multiple comparison post-test was used. n=6-12 slices. Results are from at least three independent experiments.

Fig. S3

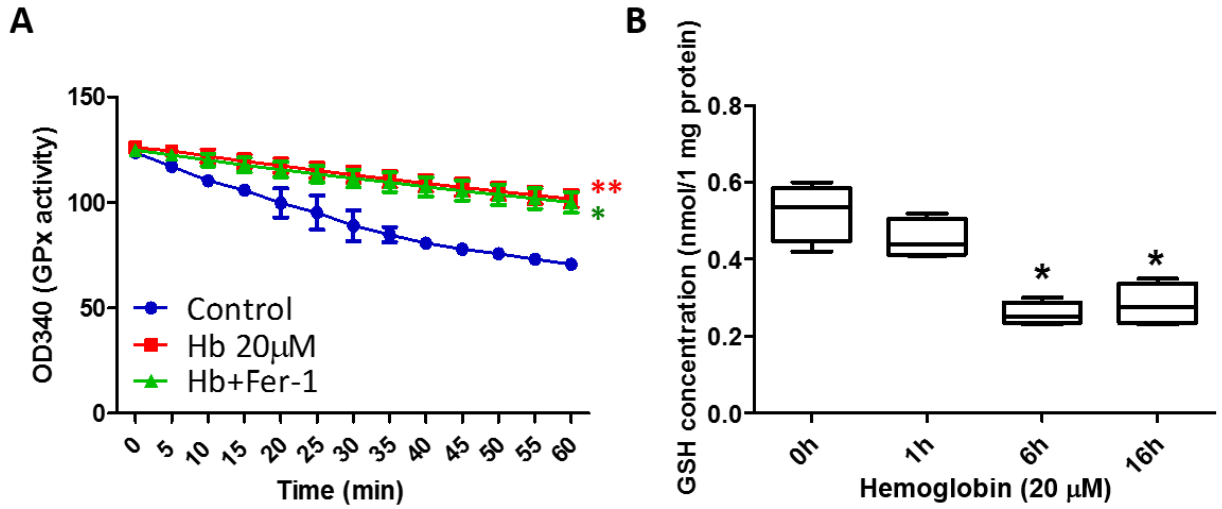

Fig. S3. Hemoglobin (Hb) exposure reduces glutathione peroxidase (GPx) activity and depletes glutathione in OHSCs. (**A**) OHSCs were treated as indicted for 4 hours, and GPx activity was examined. *p<0.05, **p<0.01 vs. Control. (**B**) OHSCs were exposed to 20 μM Hb for different time periods. Glutathione (GSH) concentration was measured with a GSH assay kit. *p<0.05 vs. Control. Results represent mean ± SD or box-and-whisker plots (the middle horizontal line within the box represents the median; boxes extend from the 25th to the 75th percentile; and the whiskers represent 95% confidence intervals). A: Repeated measurement followed by Tukey's multiple comparison; B: One-way ANOVA followed by Dunn's multiple comparison post-test. n=6-12 slices. Results are from at least three independent experiments.

Fig. S4

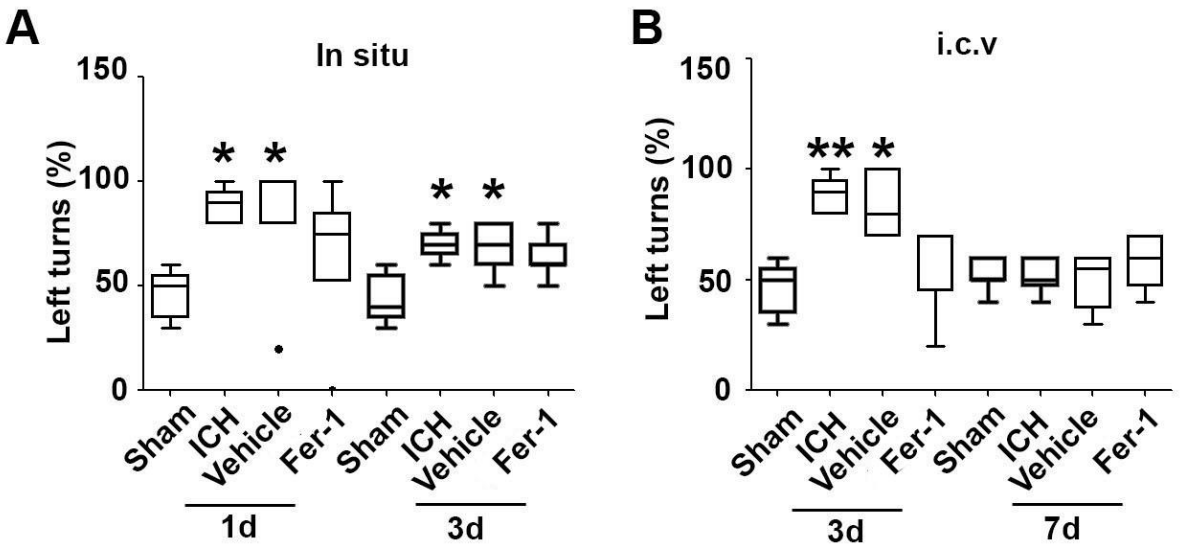

Fig. S4. Administration of Fer-1 does not correct corner turn preferences of ICH mice. Male C57BL/6 mice (8 weeks old) were injected in the left striatum with collagenase or underwent the sham procedure. Mice received an injection of Fer-1 or vehicle immediately after collagenase (*in situ* (**A**) or through the left ventricle (i.c.v.) 2 hours later (**B**). Corner turn tests were performed at 1 and 3 days. *p<0.05, **p<0.01 vs. Sham at each time point. Results are shown as box-and-whisker plots (the middle horizontal line within the box represents the median; boxes extend from the 25th to the 75th percentile; and the whiskers represent 95% confidence intervals); Kruskal-Wallis test followed by Dunn's multiple comparison post-test was used. Sham and Vehicle: n=8; ICH and Fer-1: n=10.

Fig. S5

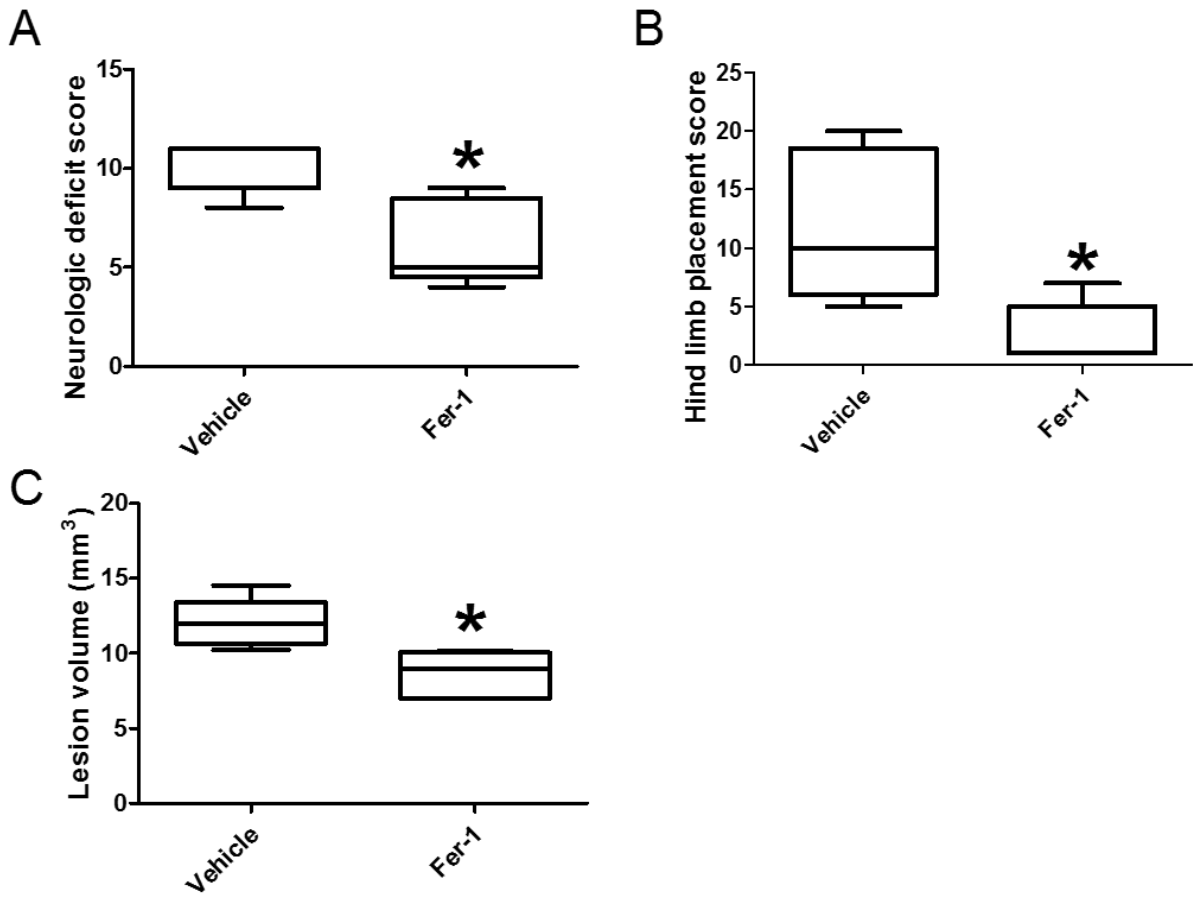

Fig. S5. Administration of Fer-1 reduces lesion volume and neurologic deficit in middle-aged male mice. Male C57BL/6 mice (12 months old) received an injection of 0.075 U collagenase in the left striatum followed 2 hours later by an injection of Fer-1 or vehicle through the left ventricle. (**A**) Neurologic deficit and (**B**) hind limb placement tests were performed after 24 hours. Mice were sacrificed, and (**C**) lesion volumes were measured by Cresyl violet/Luxol fast blue stain. Results are shown as box-and-whisker plots (the middle horizontal line within the box represents the median; boxes extend from the 25th to the 75th percentile; and the whiskers represent 95% confidence intervals). *$p<0.05$ vs. Vehicle; Wilcoxon rank sum tests (A-B) or two-tailed Student's *t*-tests (C) followed by Welch's correction. Vehicle: n=8; Fer-1: n=6.

Fig.S6

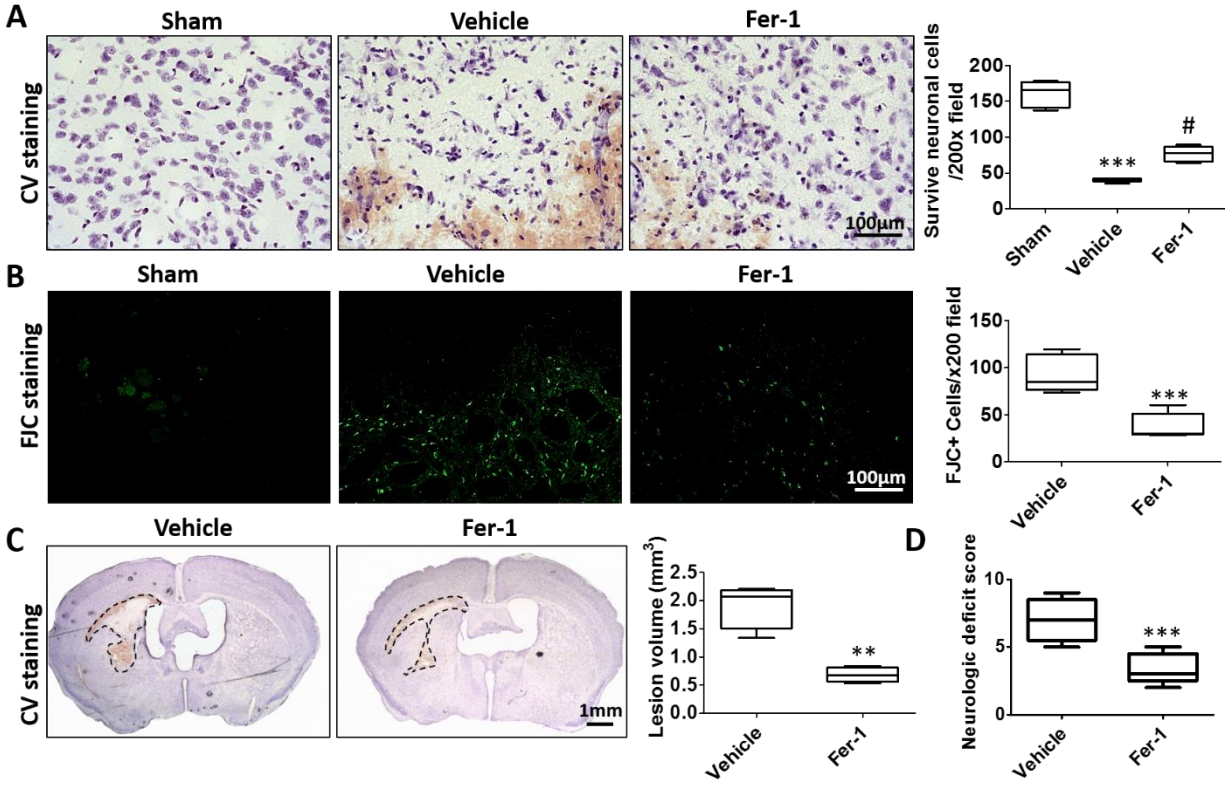

Fig. S6. Fer-1 treatment reduces neuronal death, lesion volume, and neurologic deficit in the blood injection model. Male C57BL/6 mice (2-3 months old) were injected in the left striatum with 10 µL of blood. Two hours later, they received an injection of Fer-1 or vehicle through the left ventricle. (**A**) Surviving neurons were measured by Cresyl violet (CV) stain. ***p<0.001 vs. Sham; #p<0.05 vs. Vehicle. (**B**) Fluoro-Jade C (FJC) staining was performed and quantification shown. ***p<0.001 vs. Vehicle. (**C**) Brain sections were stained with CV, and lesion volume was calculated. **p<0.01 vs. Vehicle. (**D**) Neurologic deficits were assessed after 3 days. ***p<0.001 vs. Vehicle. Results are shown as box-and-whisker plots (the middle horizontal line within the box represents the median; boxes extend from the 25th to the 75th percentile; and the whiskers represent 95% confidence intervals). A: One-way ANOVA followed by Bonferroni *post hoc*

analysis. B-D: two-tailed Student's *t*-test followed by Welch’s correction. Sham: n=10; Vehicle: n=8; Fer-1: n=10.

Fig. S7

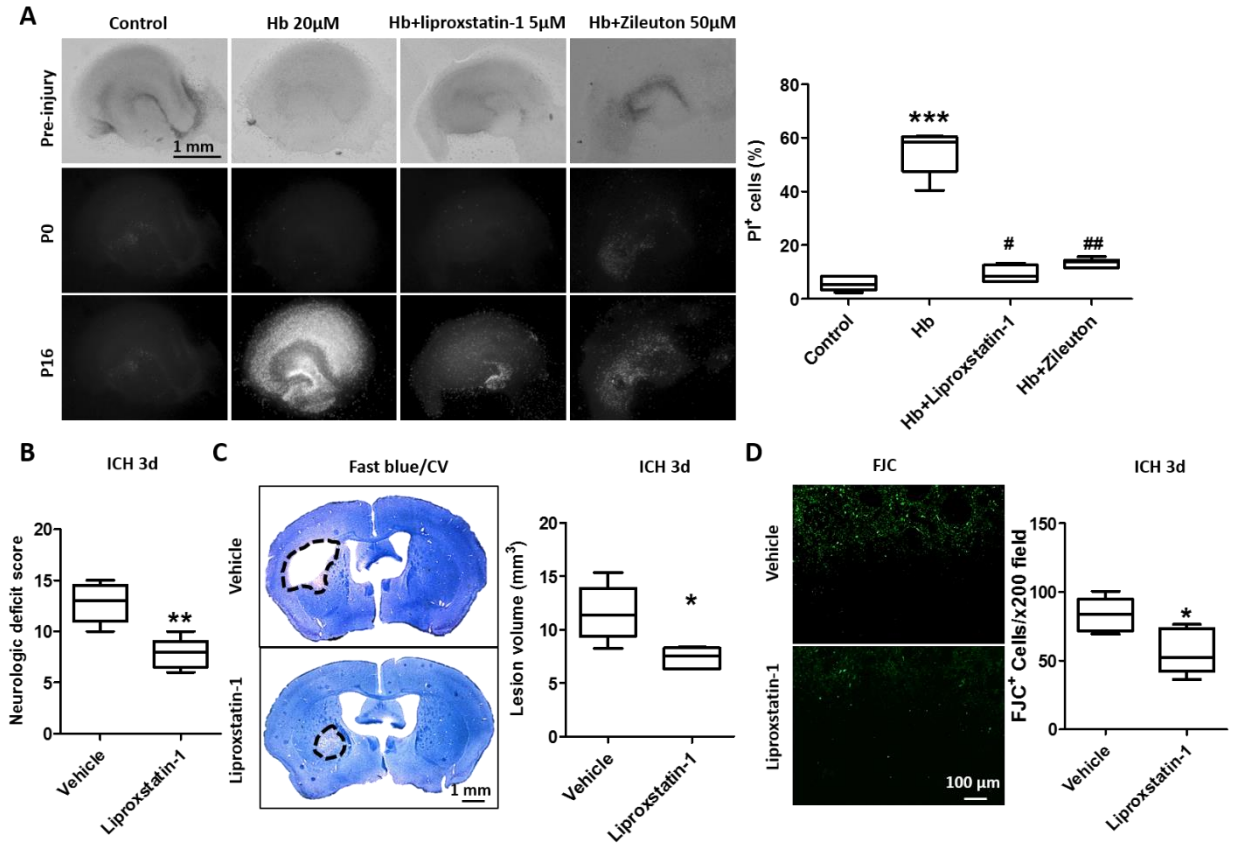

Fig. S7. Liproxstatin-1 and zileuton offer neuroprotection similar to that of Fer-1 in OHSCs and *in vivo*. (**A**) OHSCs were treated under the conditions shown for 16 hours. Slices were stained with propidium iodide (PI). Representative images and percentage of PI^+ cells are shown. Both liproxstatin-1 and zileuton reduced neuronal death compared with that in the Hb-only group. ***p<0.001 vs. Control; #p<0.05, ##p<0.01 vs. Hb. (**B-D**) Male C57BL/6 mice (8 weeks old) underwent collagenase-induced ICH. After 2 hours, they were injected intraperitoneally with liproxstatin-1 or vehicle. (**B**) At 3 days, neurologic deficit scores were lower in the liproxstatin-1–treated group than in the vehicle-treated group. Similarly, lesion volume (**C**), as calculated by Cresyl violet (CV)/Luxol fast blue staining, and neuronal death (**D**), as assessed by Fluoro-Jade C (FJC) staining, were also less in the liproxstatin-1 group than in the vehicle group. *p<0.05,

**p<0.01 vs. Vehicle. Results are shown as box-and-whisker plots (the middle horizontal line within the box represents the median; boxes extend from the 25th to the 75th percentile; and the whiskers represent 95% confidence intervals). A: One-way ANOVA followed by Dunn's multiple comparison test; results are from at least three independent experiments. B-D: two-tailed Student's *t*-test followed by Welch's correction; n=5 mice per group. Scale bars: (A) and (C) 1 mm; (D) 100 µm.

Fig. S8

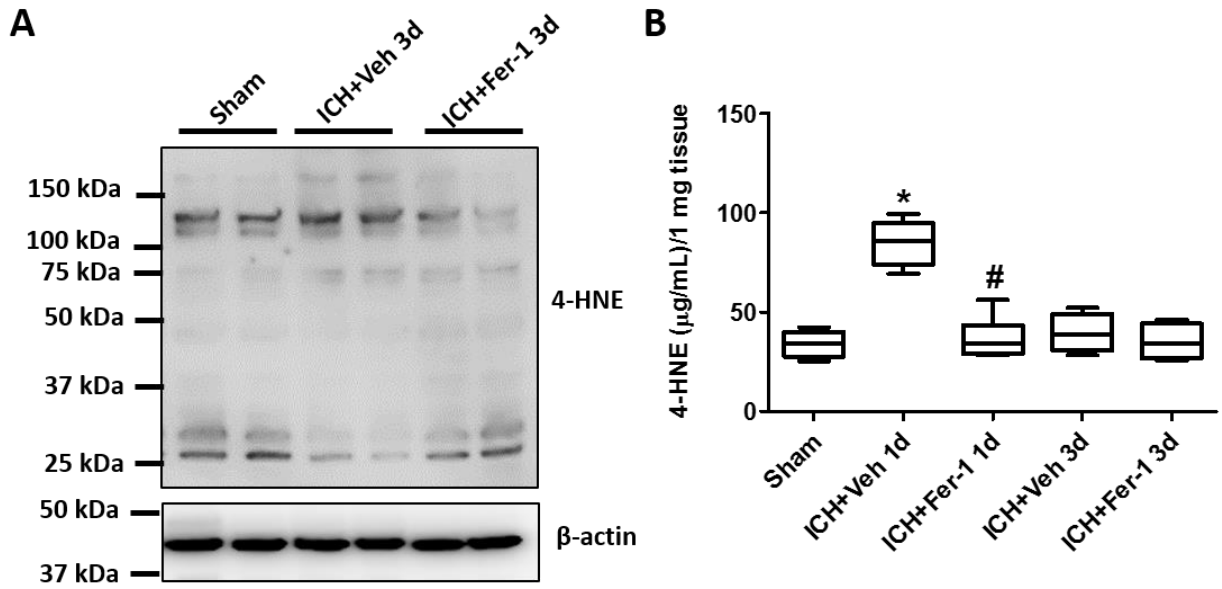

Fig. S8. Intracerebroventricular administration of Fer-1 decreases 4-hydroxynonenal (4-HNE) expression *in vivo*. Male C57BL/6 mice (8 weeks old) underwent collagenase injection or sham procedure. Fer-1 or vehicle was injected through the left ventricle 2 hours later. A 4-mm tissue slice from the hematoma core and perihematoma region was collected from all animals. Tissue was homogenized for Western blotting (**A**) and 4-HNE ELISA assay (**B**). β-actin served as a loading control. *p<0.05 vs. sham; #p<0.05 vs. ICH+Veh 1day. Results are shown as box-and-whisker plots (the middle horizontal line within the box represents the median; boxes extend from the 25th to the 75th percentile; and the whiskers represent 95% confidence intervals). B: One-way ANOVA followed by Dunn's multiple comparison post-test. Sham, ICH+Veh 1 day, and ICH+Fer-1 1 day: n=6 mice per group; ICH+Veh 3 days and ICH+Fer-1 3 days: n=4 mice per group.

Fig. S9

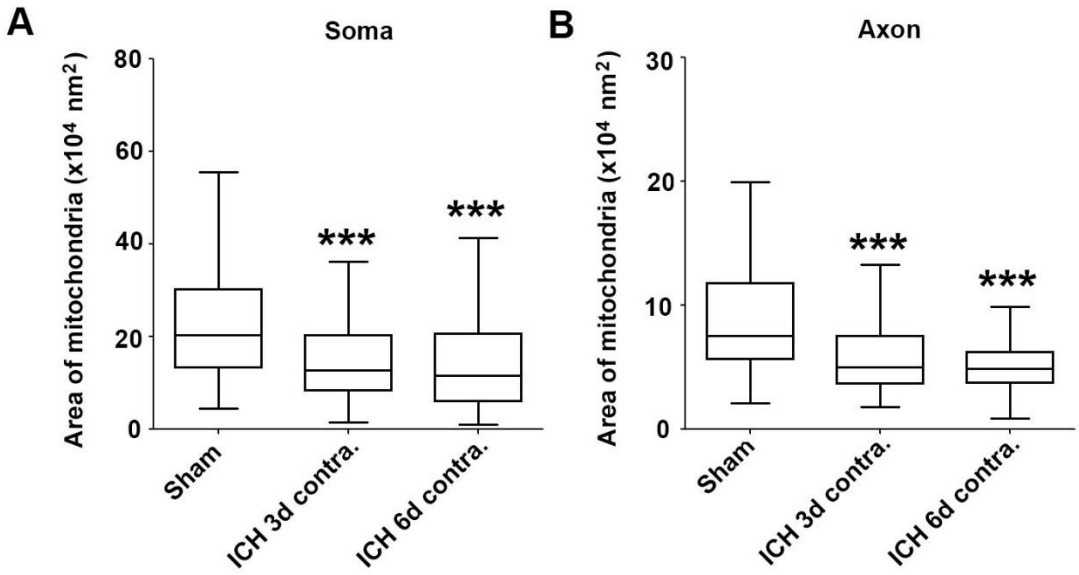

Fig. S9. Transmission electron microscopic analysis of shrunken mitochondria on the contralateral side of mouse brains. Eight-week-old male mice underwent ICH or sham procedure. The area of mitochondria in the contralateral (contra) neuronal soma (**A**) and axons (**B**) was quantified. n=3 mice per time point. (**A**) Number of mitochondria in somas, Sham = 272; ICH 3 days contra = 233; ICH 6 days contra = 309. (**B**) Number of mitochondria in axons: Sham = 152; ICH 3 days contra = 88; ICH 6 days contra = 83. **p<0.001 vs. Sham. Results are shown as box-and-whisker plots; Kruskal Wallis test followed by Dunn's *post hoc* analysis was used.

Fig. S10

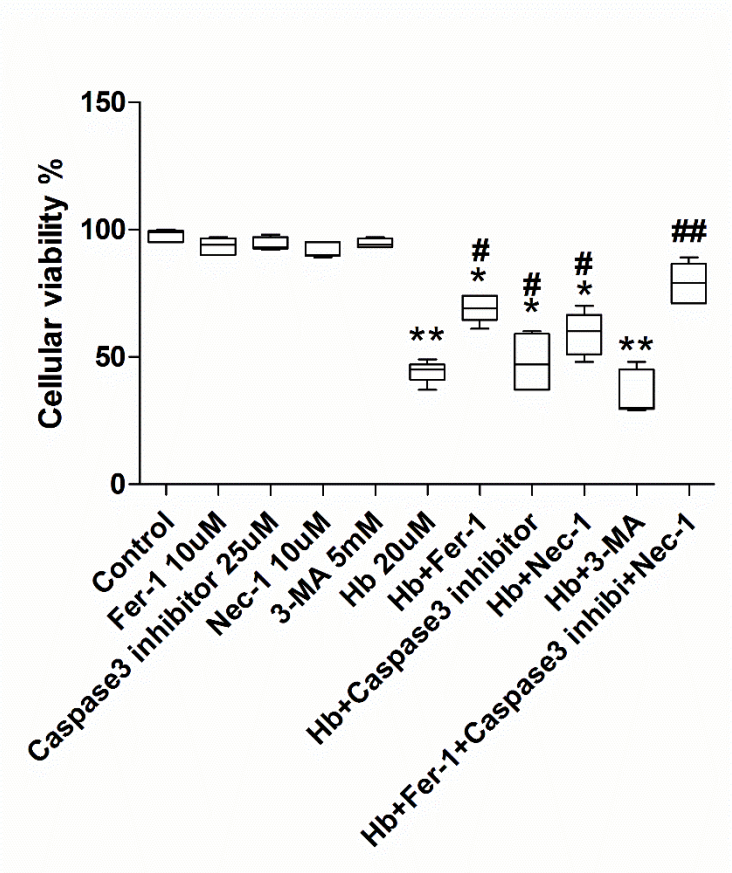

Fig. S10. Inhibiting multiple forms of cell death optimizes neuronal rescue *in vitro*. Human iPSC-derived neurons were treated as indicated for 16 hours before cell death was measured with the MTT assay. *p<0.05, **p<0.01 vs. Control; #p<0.05, ##p<0.01 vs. Hb (hemoglobin). Results are shown as box-and-whisker plots (the middle horizontal line within the box represents the median; boxes extend from the 25th to the 75th percentile; and the whiskers represent 95% confidence intervals). n=3 independent experiments; one-way ANOVA with Bonferroni *post hoc* analysis.

Fig. S11

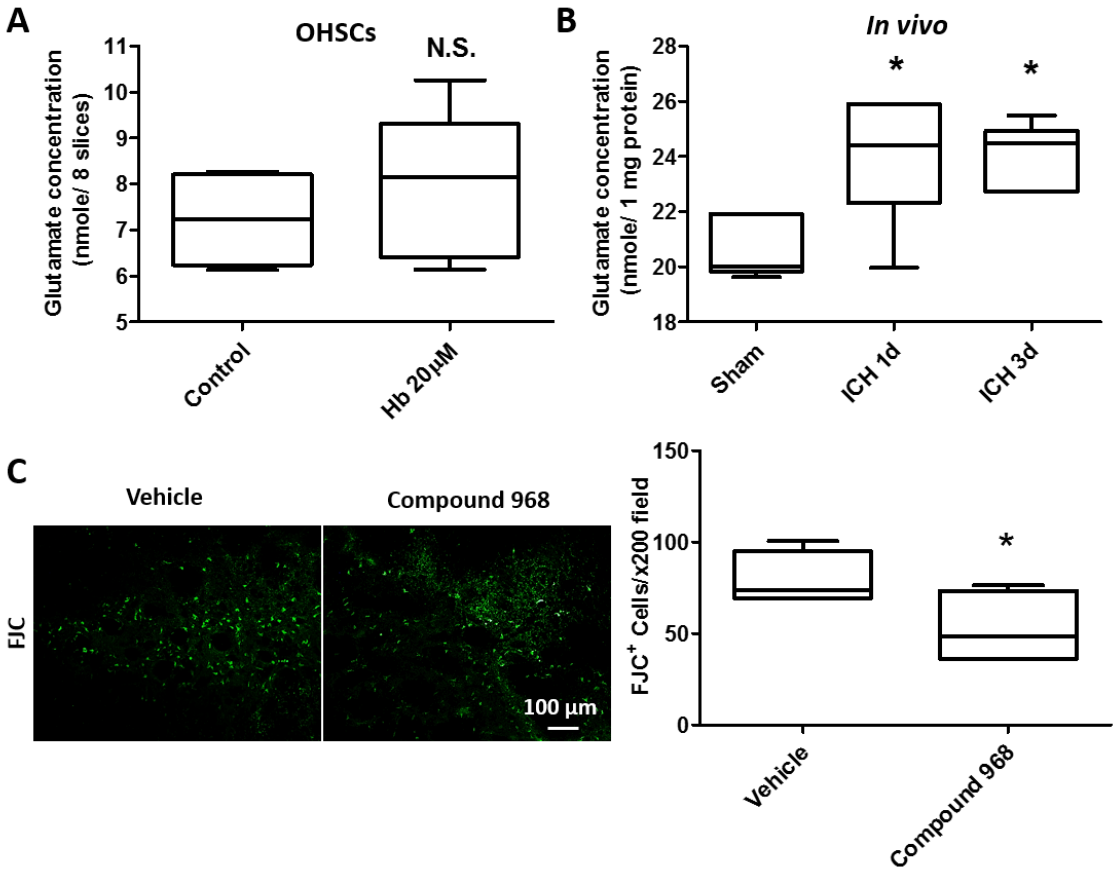

Fig. S11. ICH increases glutamate concentration, and glutaminase inhibitor compound 968 rescues neuronal death *in vivo*. (**A**) OHSCs were treated with hemoglobin (Hb) or vehicle (Control) for 16 hours. Slices were homogenized, and glutamate concentration was measured. N.S., no significance. Results are from at least three independent experiments. (**B**) Eight-week-old male mice underwent ICH or sham procedure. A 4-mm tissue slice from the hematoma core and perihematoma region was collected from ICH (1 and 3 days) and sham animals. Tissue was homogenized and glutamate concentration measured. n=5 mice per group; *$p<0.05$ vs. Sham. (**C**) Eight-week-old male mice underwent ICH. Four hours later, they were administered glutaminase inhibitor compound 968 or vehicle by intraperitoneal injection. Degenerating neurons were

measured by Fluoro-Jade C (FJC) staining at 3 days after ICH. Representative images and percentage of FJC^+ cells are shown. n=5 mice per group; *p<0.05 vs. Vehicle. Results are shown as box-and-whisker plots (the middle horizontal line within the box represents the median; boxes extend from the 25th to the 75th percentile; and the whiskers represent 95% confidence intervals). A and C: two-tailed Student's *t*-test followed by Welch's correction. B: One-way ANOVA followed by Dunn's multiple comparison post-test. Scale bars: (C) 100 μm.

Fig. S12

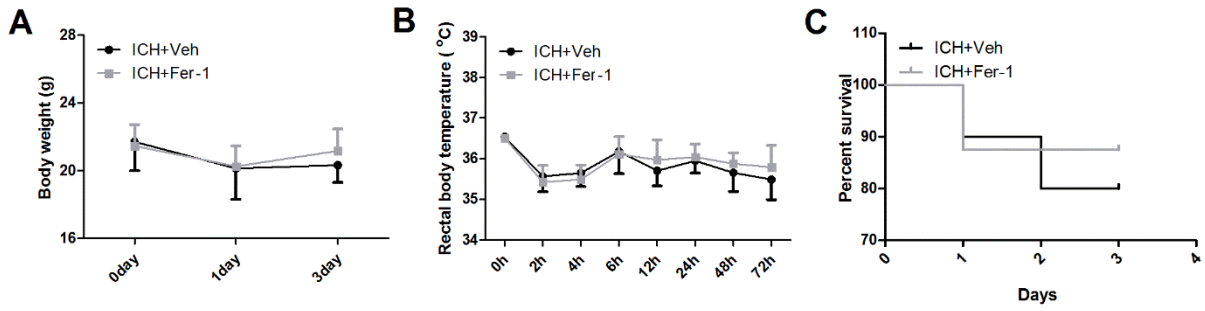

Fig. S12. *In situ* administration of Fer-1 does not change mouse body weight, body temperature, or survival curve over time. Eight-week-old male C57BL/6 mice were injected with 0.075 U collagenase followed by an *in situ* injection of Fer-1 or vehicle. (**A**) We recorded the body weight before injection (day 0) and at 1 and 3 days after injection. Body weight did not differ significantly between the vehicle-treated and Fer-1-treated groups. (**B**) We recorded the rectal temperature of mice with a rectal thermistor probe (40-90-8D DC Temperature Controller, FHC, Bowdoin, ME) before and after injection. Body temperature did not differ significantly between the vehicle-treated and Fer-1-treated groups at any time during the experimental course. (**C**) Survival curves showed no significant difference between vehicle-treated and Fer-1-treated groups. Two-way ANOVA followed by Bonferroni post-test was used for panels A and B. Data are shown as means ± SD. The log-rank (Mantel-Cox) test was used for panel C. Vehicle: n=7; Fer-1: n=9.

Fig. S13

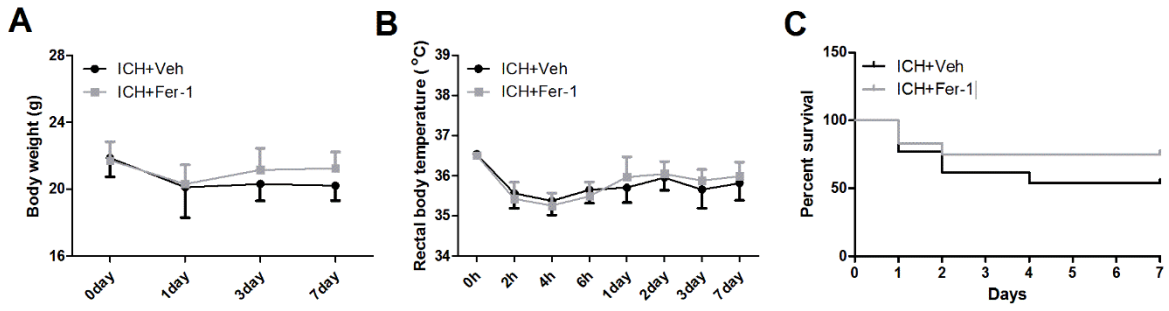

Fig. S13. Intracerebroventricular administration of Fer-1 does not change mouse body weight, body temperature, or survival curve over time. Eight-week-old male C57BL/6 mice were injected with 0.075 U collagenase followed by an intracerebroventricular injection of Fer-1 or vehicle. (**A**) We recorded body weight before injection (day 0) and at 1, 3, and 7 days after injection. Body weight did not differ significantly between the vehicle-treated and Fer-1-treated groups. (**B**) We recorded the rectal temperature of mice with a rectal thermistor probe (40-90-8D DC Temperature Controller, FHC, Bowdoin, ME) before and after injection. Body temperature did not differ significantly between the vehicle-treated and Fer-1-treated groups at any time during the experimental course. (**C**) Survival curves showed no significant difference between vehicle-treated and Fer-1-treated groups. Two-way ANOVA followed by Bonferroni post-test was used for panels A and B. Data are shown as means ± SD. The log-rank (Mantel-Cox) test was used for panel C. Vehicle: n=7; Fer-1: n=9.

Supplementary methods and materials

Striatal slice cultures

We prepared organotypic striatal slice cultures according to the methods described previously (1). Briefly, C57BL/6 mouse pups (P7-P9) were decapitated and each hemisphere was cut into coronal slices of 300-μm thickness under sterile conditions. Slices containing the parietal cortex and the striatum were chosen, and the other brain structures were removed from each slice. Corticostriatal slices were transferred onto a hydrophilic PTFE cell culture insert and cultured in 50% DMEM, 25% heat-inactivated horse serum, 25% HBSS, and 6.5 mg/mL glucose. Medium was changed every 2–3 days. After 10–14 days of culture *in vitro*, the sections were placed in serum-free medium (75% DMEM).

LDH activity assay

The activity from samples was measured by using an LDH activity assay kit (Sigma). Briefly, medium from treated slices or cells was collected and centrifuged. Then the samples were incubated with substrate and assay buffer in a clear 96-well plate. LDH in the samples reduced NAD to NADH, which was specifically detected at 450 nm with a plate reader (Spectramax M2 microplate reader; Molecular Devices LLC, Sunnyvale, CA).

ROS measurement

OHSCs were incubated with 63 μM HEt (Invitrogen) for 30 minutes (2) before images were captured under a fluorescence microscope ((Nikon Eclipse 90i). An investigator blinded to treatment measured fluorescence intensity using Image J software.

Reverse transcription and real-time PCR

Total mRNA was extracted from OHSCs by QIAzol Lysis Reagent (miRNeasy Mini Kit; QIAGEN, Gaithersburg, MD). One microgram of RNA from each sample was transcribed into cDNA with the SuperScript VILO cDNA Synthesis Kit (Invitrogen). Real-time PCR was performed on an ABI 7500 Fast Real-Time PCR System (Applied Biosystems, Foster City, CA) in TaqMan Universal PCR master mixture II with uracil N-glycosylase (Applied Biosystems). The following TaqMan Gene Expression Assay Mixes (Applied Biosystems) were used: *ATP5G3* (Mm01334541_g1), *IREB2* (Mm01179595_m1), *RPL8* (Mm00657299_g1), *CS* (Mm00466043_m1), and *PTGS2* (Mm00478374_m1). The endogenous control was *GAPDH* (Mm99999915_g1). The cycle time values of candidate genes were normalized to *GAPDH* in the same sample. The expression levels of mRNA were then presented as fold change versus control as previously described (3).

Quantification of FJB/FJC, CV, and Perls' staining

FJB/FJC, CV, and Perls staining were quantified on sections at 1.70, 0.74, and -0.34 mm from the bregma. Three sections per animal were viewed and photographed under a microscope by an investigator blinded to group. FJB- and CV-stained healthy neurons (with nuclei) and Perls-stained iron-positive cells were counted by sampling an area of 500 × 1000 μm^2 immediately adjacent to the hematoma in three randomly selected fields at 200× magnification in each section. The ROI was defined within one 20× field that corresponded to ~460 μm from the edge of the hematoma. Healthy neurons and iron-positive cells were expressed as cells/200× field (4).

Stereology

In a subset of mice used for calculating lesion volume at day 7 after ICH, we performed unbiased stereology on the ipsilateral striatum according to the protocol by Yang *et al.* (5) with slight changes. Stereological measurements were made with a Nikon Eclipse 90i microscope (Nikon, Tokyo, Japan) attached to a Qimage Retiga-2000R camera, which was connected to a workstation with Stereo Investigator software (Version 10; MicroBrightField, Williston, VT). A set of CV-stained sections was selected at random from every 12 evenly spaced sections (120 μm apart) of the entire ipsilateral striatum (Bregma: 1.70 mm ~ -2.12 mm). The optical dissector height (thickness) was 12 μm with a 2-μm top and bottom guard zone. We sampled 10–15 counting frames per section and counted 10–15 neurons per frame. A viable neuron could be distinguished from glia based on its size, presence of a visible rim of cytoplasm around the nucleus, and a prominent nucleolus. A neuron was counted only when its nucleus first came into focus within the optical dissector counting frame. It was not counted if the nucleus came into focus within the guard zone or was touching the left or bottom side of the dissector frame. The mean section thickness, measured at every counting frame site, was used for final calculation of the number of neurons in the striatum.

MTT assay

Cell number was measured with an MTT proliferation assay kit (Life Technologies). Cells were seeded at a density of 5000–10,000 per well in a 96-well plate. After different treatments, cells were incubated with 12 mM MTT reagent for 4 hours. SDS-HCl was then added for another 4 hours at 37°C. The sample was mixed by a pipette, and absorbance was measured at 570 nm.

Glutathione concentration measurement

Glutathione concentration was measured with a glutathione assay kit (Abcam). Briefly, treated slices were removed from the insert membrane in cold PBS, lysed by homogenization in buffer containing 1 mM EDTA, and centrifuged at 10,000*g* for 15 minutes at 4°C. Concentration of glutathione in the supernatant was measured by reacting glutathione with DTNB [5,5'-dithiobis(2-nitrobenzoic acid)]. Optical density was measured at 412 nm.

Glutamate concentration measurement

Glutamate concentration was measured by a glutamate assay kit (Abcam). Briefly, treated slices, 4-mm ipsilateral striatum including hematoma core and perihematomal region, or corresponding brain tissue from control mice was harvested and homogenized with assay buffer. Sample was incubated on ice for 15-30 minutes and then centrifuged at 10,000*g* for 15 minutes at 4°C. The supernatant was mixed with assay buffer, developer, and glutamate enzyme mix for 30 minutes at room temperature and protected from light. The glutamate enzyme mix recognizes glutamate as a specific substrate leading to proportional color development. The amount of glutamate can therefore be quantified by the colorimetric assay at 450 nm.

References

1. Fujimoto S, Katsuki H, Kume T, and Akaike A. Thrombin-induced delayed injury involves multiple and distinct signaling pathways in the cerebral cortex and the striatum in organotypic slice cultures. *Neurobiol Dis.* 2006;22(1):130-42.
2. Kovacs R, Schuchmann S, Gabriel S, Kann O, Kardos J, and Heinemann U. Free radical-mediated cell damage after experimental status epilepticus in hippocampal slice cultures. *J Neurophysiol.* 2002;88(6):2909-18.
3. Li Q, Wijesekera O, Salas SJ, Wang JY, Zhu M, Aprhys C, Chaichana KL, Chesler DA, Zhang H, Smith CL, et al. Mesenchymal stem cells from human fat engineered to secrete BMP4 are nononcogenic, suppress brain cancer, and prolong survival. *Clin Cancer Res.* 2014;20(9):2375-87.
4. Chang CF, Cho S, and Wang J. (-)-Epicatechin protects hemorrhagic brain via synergistic Nrf2 pathways. *Ann Clin Transl Neurol.* 2014;1(4):258-71.
5. Yang ZJ, Wang B, Kwansa H, Heitmiller KD, Hong G, Carter EL, Jamrogowicz JL, Larson AC, Martin LJ, and Koehler RC. Adenosine A2A receptor contributes to ischemic brain damage in newborn piglet. *J Cereb Blood Flow Metab.* 2013;33(10):1612-20.

Full unedited gel for Figure 5F **4-HNE**

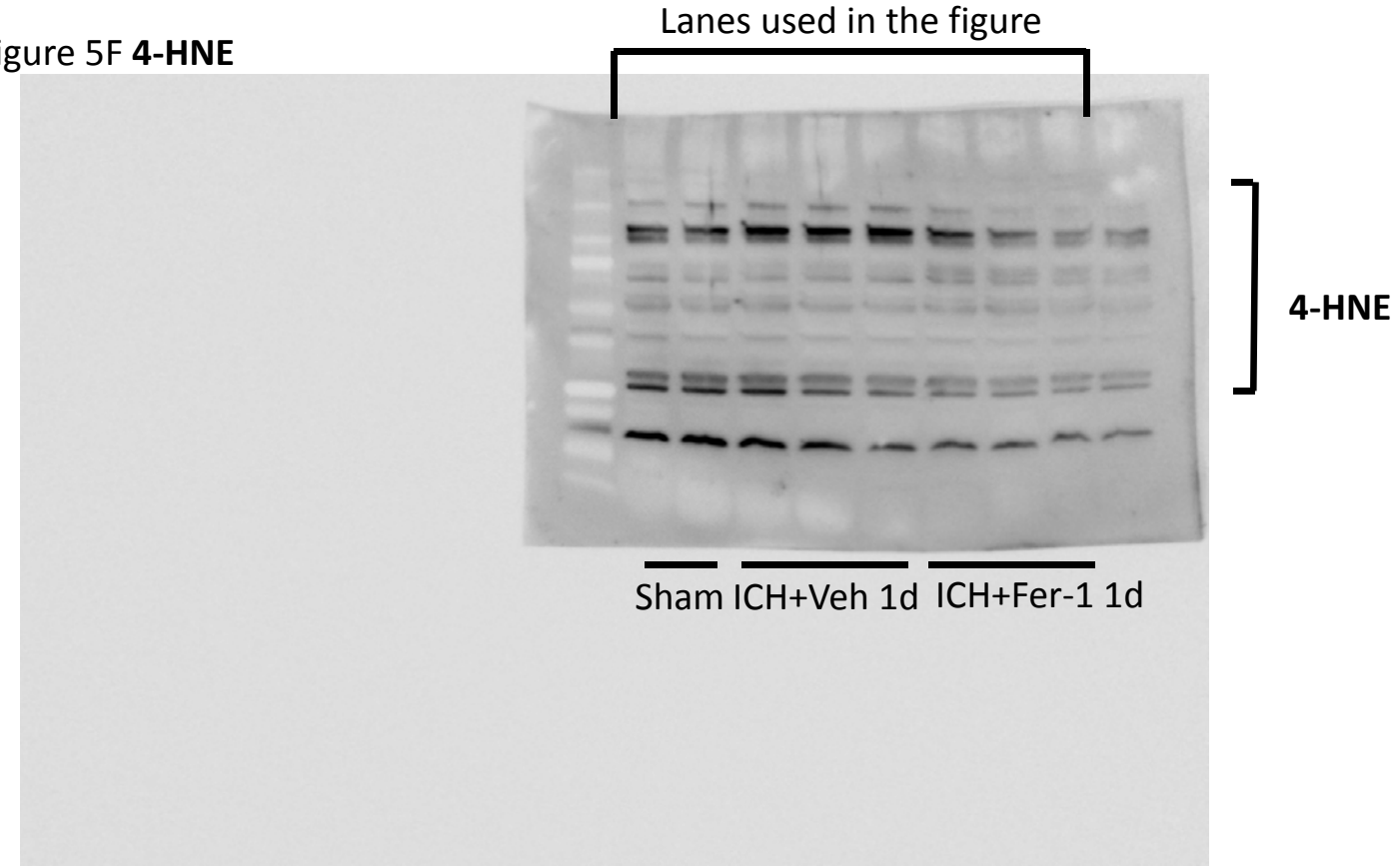

Full unedited gel for Figure 5F **β-actin**

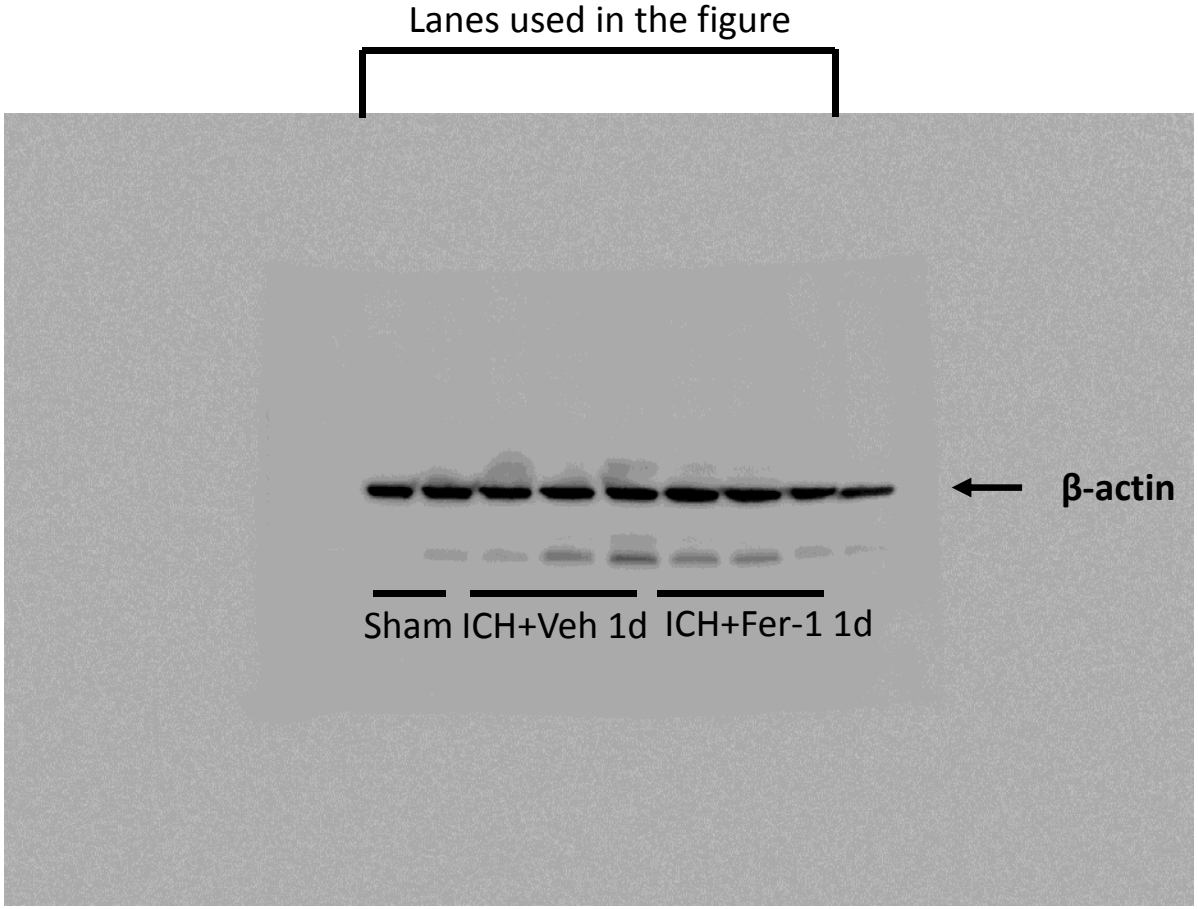

Full unedited gel for Figure 5G **COX-2**

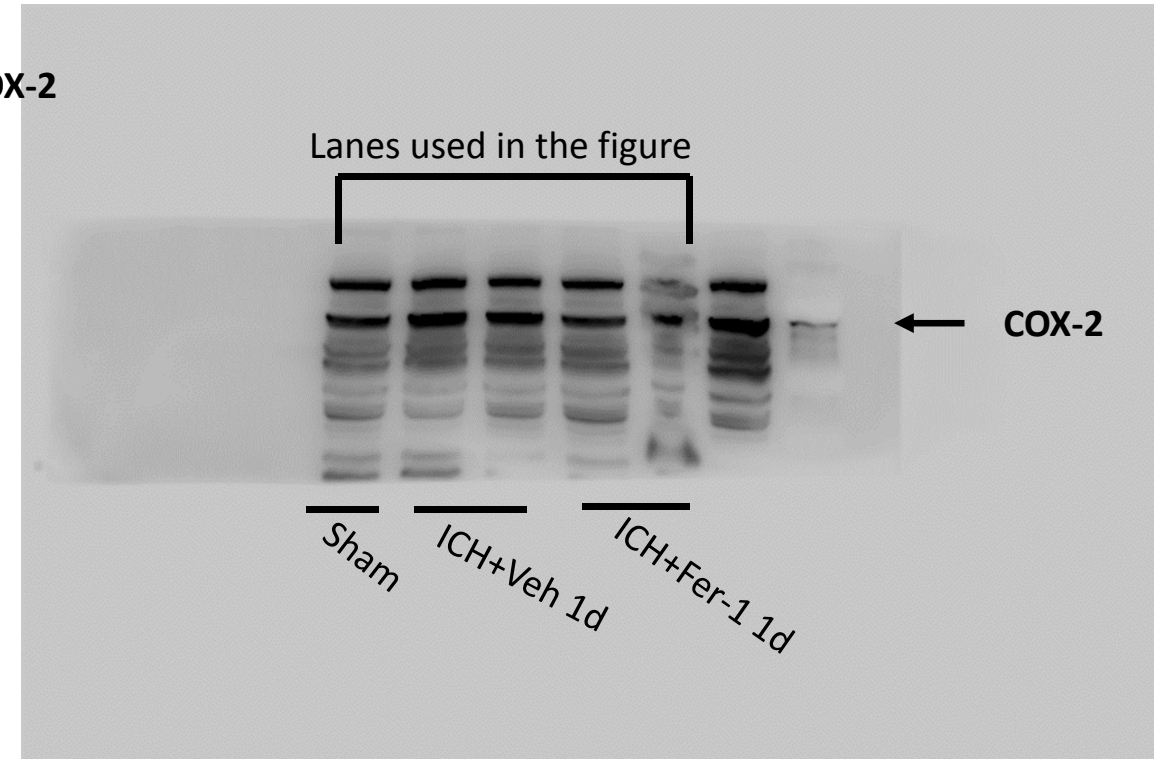

Full unedited gel for Figure 5G **β-actin**

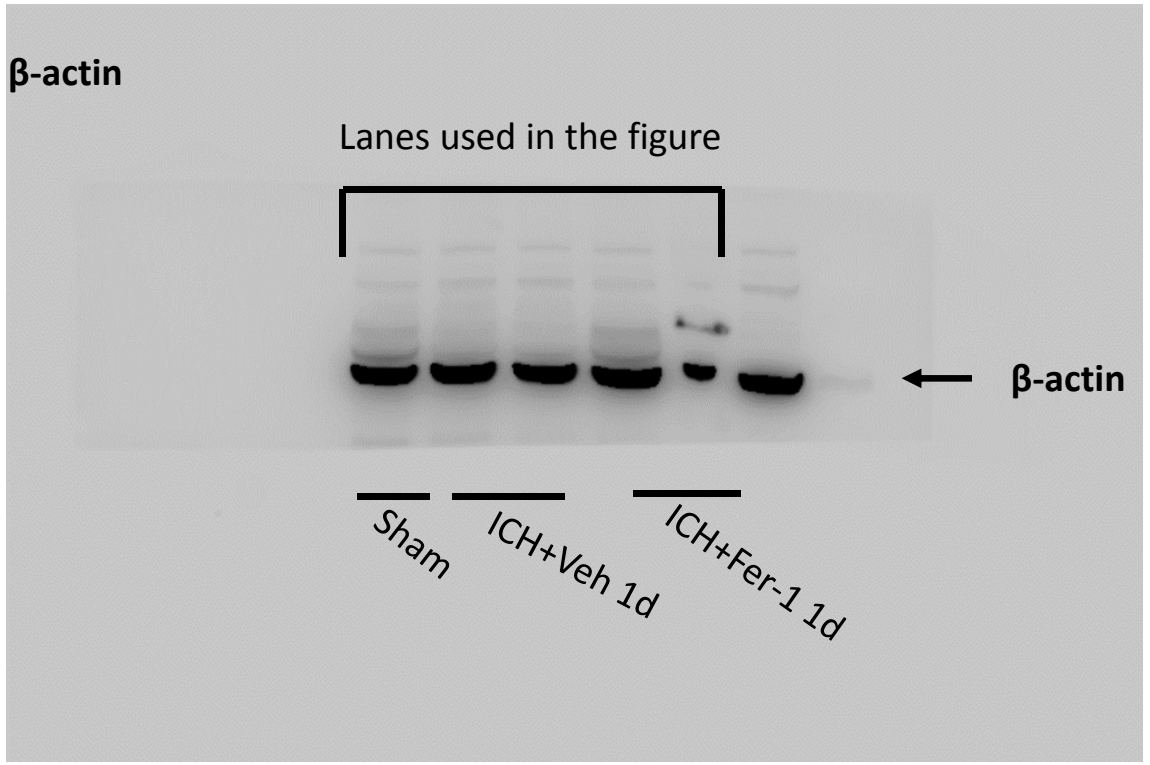

Full unedited gel for Figure S8A **4-HNE**

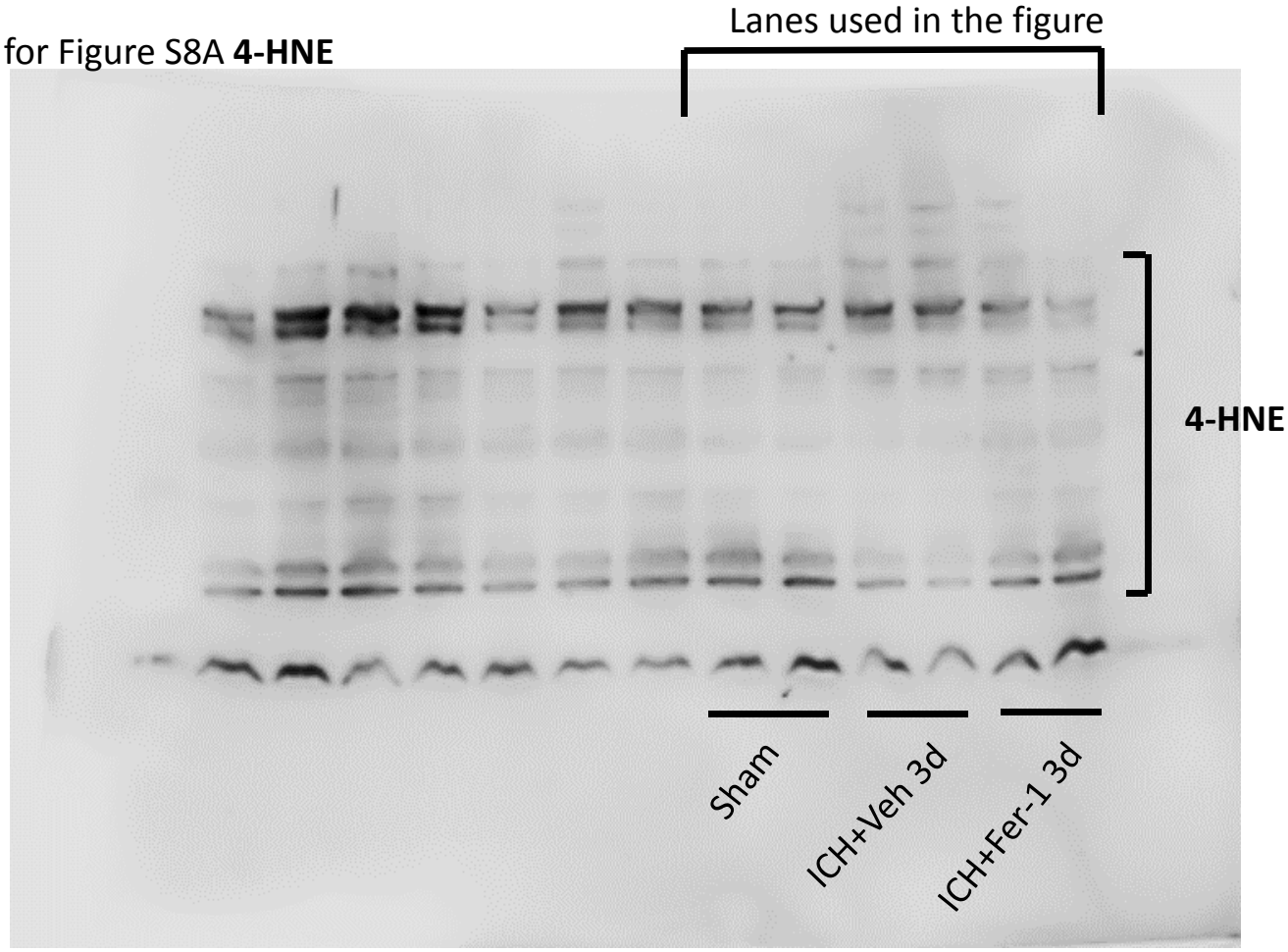

Full unedited gel for Figure S8A **β-actin**

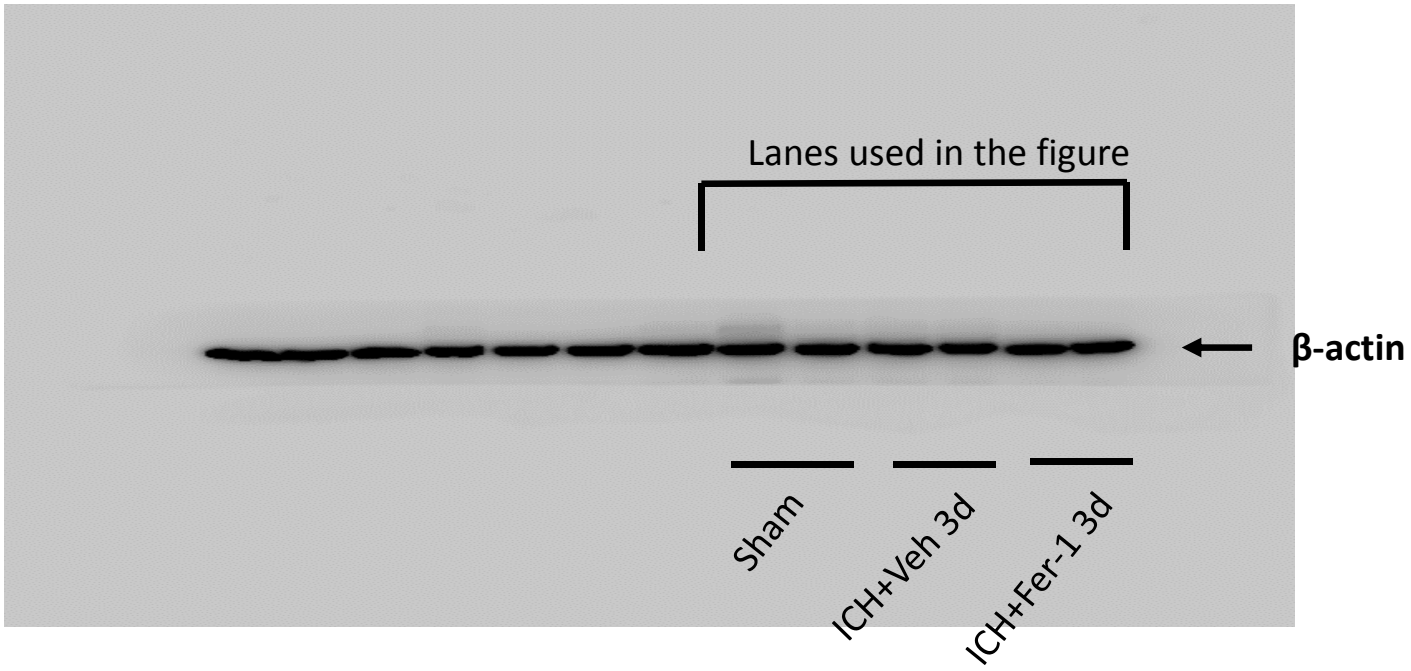

Full unedited gel for Figure S1C **NeuN**

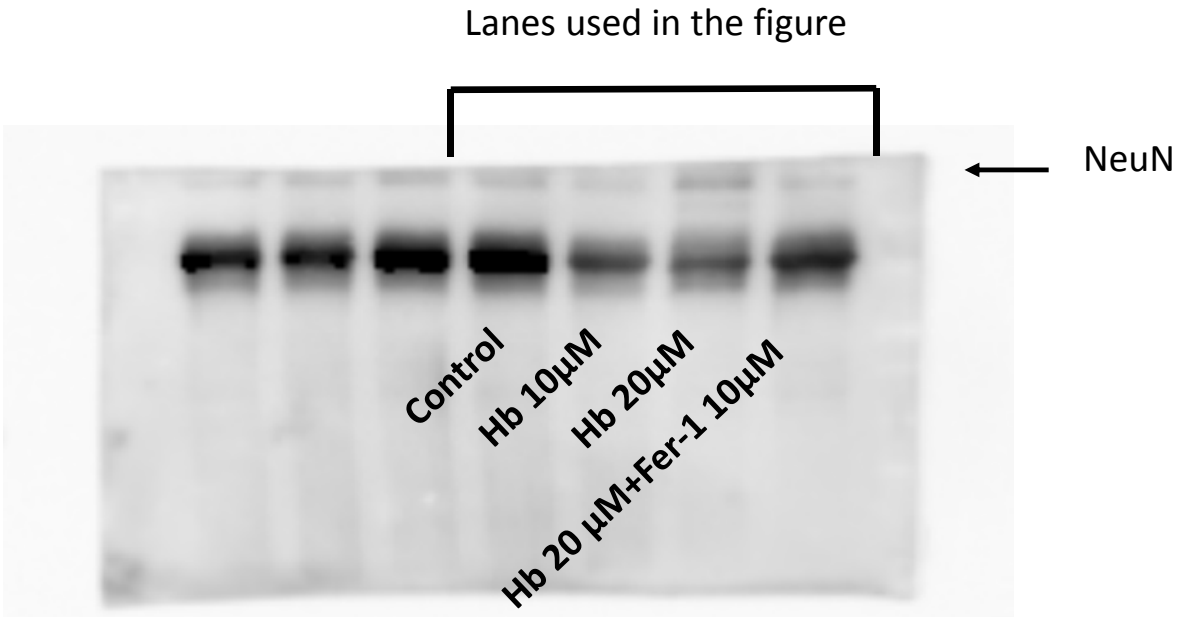

Full unedited gel for Figure S1C **Cleaved caspase-3**

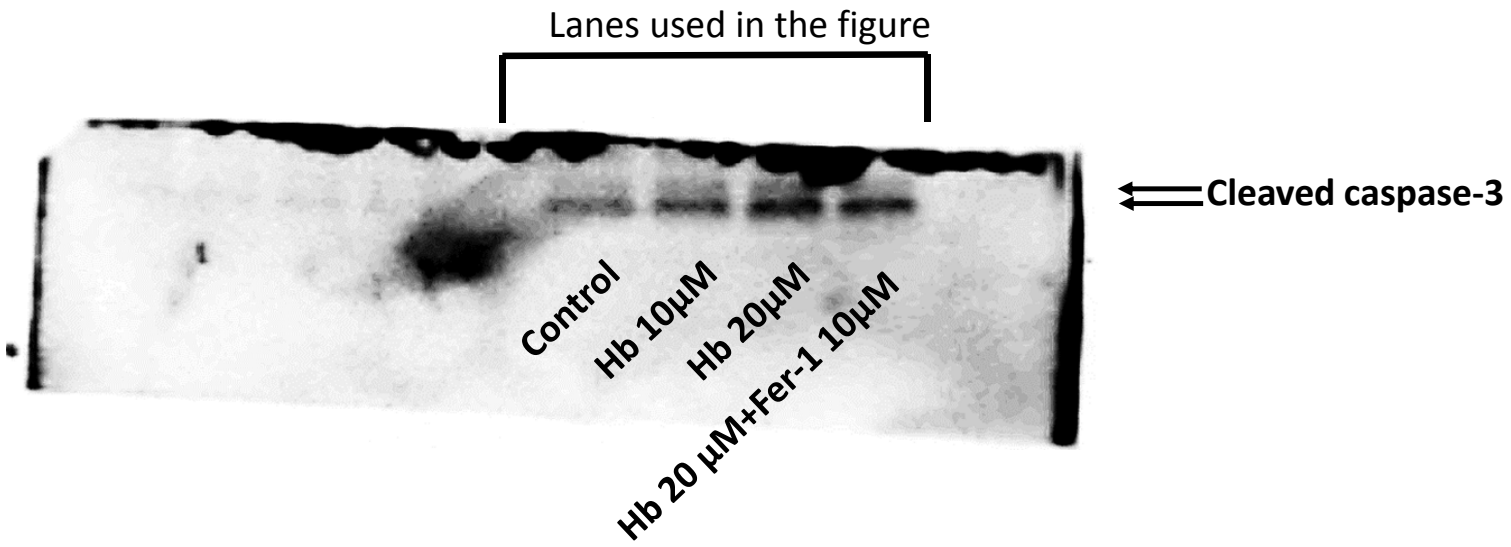

Full unedited gel for Figure S1C **β-actin**